Honors Thesis:
Characterizing the Role of the Zinc Responsive Protein, MTF-1, in Cellular Zinc Transport and Proliferation

Kylie Conway
October 29, 2020

Thesis Advisor:
Dr. Amy Palmer (Department of Biochemistry)

Committee Members:
Dr. Christy Fillman (Department of Molecular, Cellular and Developmental Biology)
Dr. Alison Vigers (Department of Psychology)

University of Colorado Boulder
Department of Molecular, Cellular and Developmental Biology
Fall 2020

Table of Contents:

Abstract

Zinc is the second most abundant transition metal in the human body and both increased and decreased levels of labile (cytosolic unbound) Zn^{2+} have been implicated in many different disease states including Alzheimer's disease and some forms of cancer (Quin 2011, James 2017, Rosa 2019). MTF-1 (metal regulatory transcription factor 1) is a transcription factor that has been shown to activate proteins that mediate high concentrations of labile Zn^{2+} via sequestration and enhancement of Zn^{2+} export (Jackson 2020). In this study, MTF-1 was knocked down in mammary epithelial cells and the labile zinc concentrations in both knockdown and control conditions were measured by fluorescence microscopy utilizing Zap-CV2 sensor. Cellular proliferation and death in different zinc conditions was also measured via cell counting. Based on the results of this study, MTF-1 knockdown resulted in higher labile zinc concentrations. Additionally, MTF-1 knockdown resulted in decreased cellular proliferation and increased cell death in the presence of higher concentrations of zinc.

Introduction

Zinc and Human Health

Zinc is a vital micronutrient that is integral in a variety of cellular functions including catalysis and regulation of everyday processes (Roohani 2013). Because of its wide variety of uses throughout the body, dietary zinc consumption is vital to maintain proper functioning of biological systems, and a lack of zinc can result in a host of negative health outcomes (Roohani 2013). This clinical lack of dietary zinc intake is known as zinc deficiency, and it affects much of the world, especially communities whose diets consist primarily of cereals and consume little red meat (Roohani 2013). In 2012, it was estimated that 17.3% of the world's population is at risk of zinc deficiency, and the World Health Organization estimates that 33% of the world's population is consuming less than the recommended amount of zinc (Wessells 2012; Lo 2020). Minimal zinc over time can result in cognitive impairment due to inefficient cell signaling and overall less efficient immune responses (Prasad 2013). Additionally, a lack of zinc during vital growth phases such as childhood, puberty, and pregnancy results in stunting of growth and development (Roohani 2013; Prasad 2013). On the cellular level, zinc deficiency results in a failure of cells to divide and multiply normally, resulting in a wide variety of health and growth problems (Vallee 1993).

A decrease in zinc levels, specifically the unbound zinc ion (Zn^{2+}) has been observed in disease states such as cancer, Parkinson's disease and prostate disease (Zowczak 2001; Rosa 2019; Zhao 2016; Kocaturk 2000). Additionally, elevated zinc levels have been found in other disease states such as Alzheimer's and chronic kidney disease (James 2017; Pelletier 2014). These diseases displaying abnormal zinc levels demonstrate the importance of identifying cellular mechanisms of zinc regulation. The Palmer lab recently showed that zinc is explicitly required in two places in the cell cycle: beginning of G1 (also known as general growth phase) and in the S phase (the phase in which DNA is replicated), demonstrating that cytosolic zinc concentration plays a part in cell cycle regulation (Lo 2020). Additionally, they found that zinc deficiency induces quiescence, or a temporary exit from the cell cycle, and that replenishing the zinc resulted in cell cycle reentry (Lo 2020). Given that altered zinc is associated with disease and can also interfere with normal cellular processes such as the cell cycle, it is important to better understand how cells regulate this essential ion.

Cellular Zinc Transport

The host of health problems associated with zinc deficiency combined with the fact that zinc is the second most prevalent transitional metal in humans implies the necessity of the presence of a steady source of Zn^{2+} in the cell (Quin 2011). In fact, Zn^{2+} is a cofactor for approximately 10% of human proteins, and is vital for carrying out many cellular processes including secretion, transcription, and DNA synthesis and repair (Andreini 2006). Unfortunately, Zn^{2+} is a heavy metal, so excessive amounts of Zn^{2+} can result in cell death (Gunther 2012). Since Zn^{2+} is necessary in small quantities for so many processes, it is important for the cell to tightly regulate the concentration of cytosolic Zn^{2+} in order to function to its full potential.

Cells are known to contain specific transporters that control labile Zn^{2+} ions into and out of the cell in order to maintain homeostasis. The family that controls Zn^{2+} influx is known as the

ZIP/SLC39 family and mediates Zn^{2+} entry into the cytosol via facilitated diffusion (Huang 2012). ZIPs are transmembrane proteins that are present in both organellar membranes as well as the cell membrane in order to increase the concentration of labile Zn^{2+} in the cytosol when the available Zn^{2+} becomes too low (Jeong 2013). The intake of Zn^{2+} via ZIP transporters is balanced by enabling Zn^{2+} removal from the cytosol, which is made possible by members of the ZnT/SLC30 family. ZnTs work to transport Zn^{2+} out of the cytosol when the concentration of labile Zn^{2+} is too great.

      The ZnTs relevant for this study are ZnT1 and ZnT2. ZnT1 is known to be expressed in nearly all cell types and is the main Zn^{2+} exporter for the cell (Dong 2015). ZnT2 is responsible for sequestration of excess Zn^{2+} into vesicles, and is upregulated in high cellular Zn^{2+} conditions in order to prevent cytotoxicity (Lee 2015). As with all passive transporters, the effectiveness of the channel is directly proportional to the quantity of ZnT1s present on the cellular membrane, and therefore there must be a mechanism by which the ZnT1 gene can be transcriptionally activated (Augustine 2018). MTF-1 (metal regulatory transcription factor 1) contains six zinc fingers that are highly conserved, each containing a different affinity for Zn^{2+} (Jackson 2020, Gunther 2012). When excess zinc binds to these regions a conformational change occurs exposing a nuclear localization sequence, and MTF-1 is able to translocate into the nucleus to activate gene expression (Gunther 2012). It is known that Zn^{2+}-bound MTF-1 is able to increase expression of ZnT1 and ZnT2 via binding to each gene's MRE (metal responsive element) region (Dong 2015). Additionally, MTF-1 activates expression of metallothionein (MT), which is able to sequester free metal ions, such as Zn^{2+} in the cell (Jackson 2020). **Figure 1** illustrates a simplified version of relevant parts of this MTF-1-ZnT1-ZnT2-MT pathway.
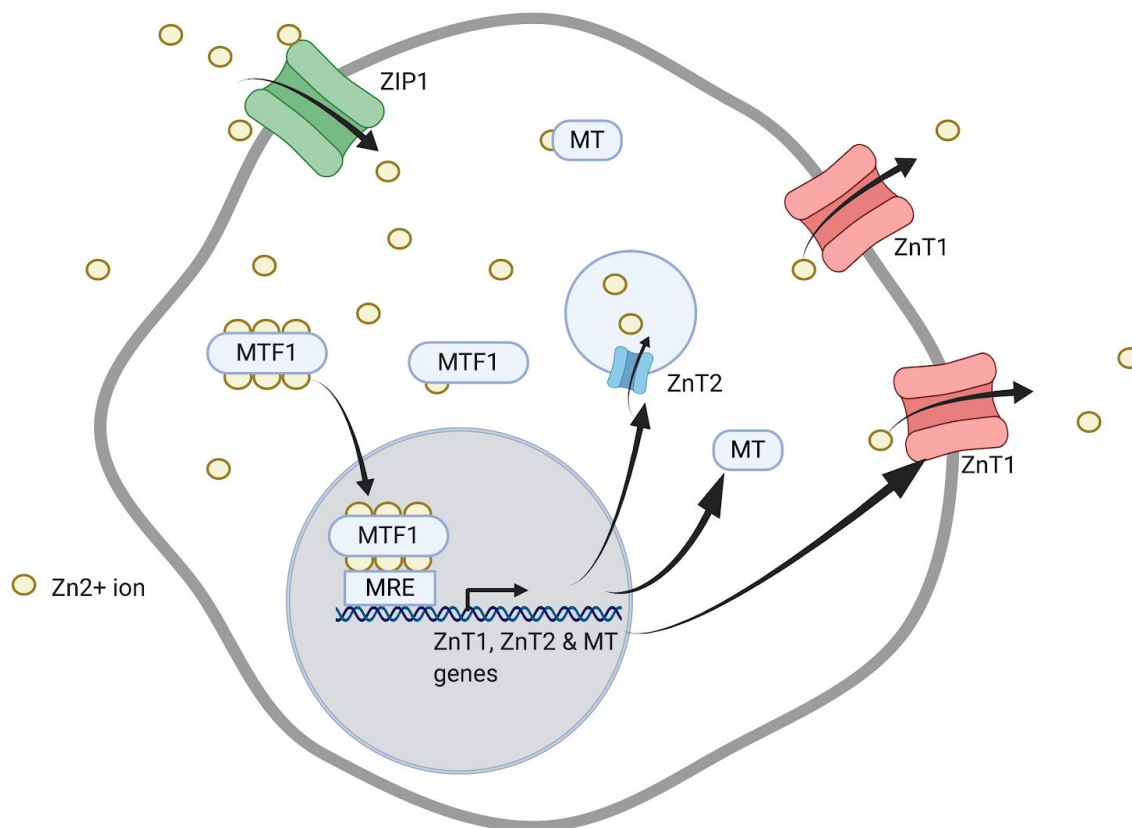
Figure 1: Zn-bound MTF-1 enhances transcription in presence of excess labile Zn. Each yellow dot represents a Zn^{2+} ion. When ZIP1 imports an excess of Zn^{2+} ions into the cytosol, MTF-1 is able to weakly bind to up to 6 Zn^{2+} ions. Zn^{2+} binding results in a conformational change exposing a NLS (nuclear localization sequence) resulting in translocation of the complex into the nucleus (Gunther 2012). The MTF-1-Zn complex is then able to bind to a metal responsive element (MRE) which enhances expression of Zn^{2+} exporter ZnT1 as well as Zn^{2+} sequestering elements metallothionein (MT) and ZnT2 (Dong 2015, Jackson 2020). Note that each gene does have a different MRE that MTF-1 can bind to, the diagram does not reflect this for simplification. *Figure generated via BioRender.com.*

Measuring cellular Zinc concentration via fluorescence microscopy

To study the role of ions in the cell, a wide variety of tools have been developed in order to quantify ion concentrations. Secondary ion mass spectrometry (SIMS), laser ablation inductively coupled plasma mass spectrometry (LA-ICP-MS), and electron spectroscopy imaging (ESI) have been used in order to identify the total concentration of a given ion in the cell; however, they are unable to distinguish between bound and unbound metal ions (Dean 2012). Other techniques are able to quantify binding of a metal ion via a visual indication, some methods include: fluorescence, phosphorescence, luminescence, or magnetic resonance imaging (MRI) (Dean 2012).

One of the tools that has been developed to measure zinc concentrations via fluorescence is known as the Zap-CV2 sensor. Zap-CV2 consists of a cyan fluorescent protein (CFP) linked to a yellow fluorescent protein (YFP) via a zinc binding domain containing the first two zinc

fingers of Zap1 transcription factor (see **Figure 2**) (Fielder 2017). This genetically encoded sensor utilizes FRET (fluorescence resonance energy transfer), a process by which energy is transferred from one fluorophore to another via dipole-dipole interactions (Sekar 2003). In the case of Zap-CV2, this energy transfer can only occur when zinc is bound to the sensor's zinc binding domain, resulting in a conformational change that results in the two fluorescent proteins moving close enough together for efficient transfer to occur (Carpenter 2016). When zinc is unbound, the CFP fluoresces, and when zinc is bound, the YFP fluoresces (Fielder 2017). When the sensor is illuminated at the right wavelength for the CFP region, an electron is able to transfer to the YFP excited level if the YFP is close enough. As the electron moves back to a resting state, a photon is emitted resulting in fluorescence of the YFP. The ratio of bound to unbound sensor can be used to determine the dissociation constant or KD of the sensor, and from there the concentration of cytosolic zinc can be determined. In order to measure only cytosolic zinc and exclude organellar or nuclear zinc, a nuclear exclusionary sequence (NES) was added to the Zap-CV2 sensor. In the case of this research, the NES Zap-CV2 was inserted into the genome via PiggyBAC transposon system (Fielder 2017).
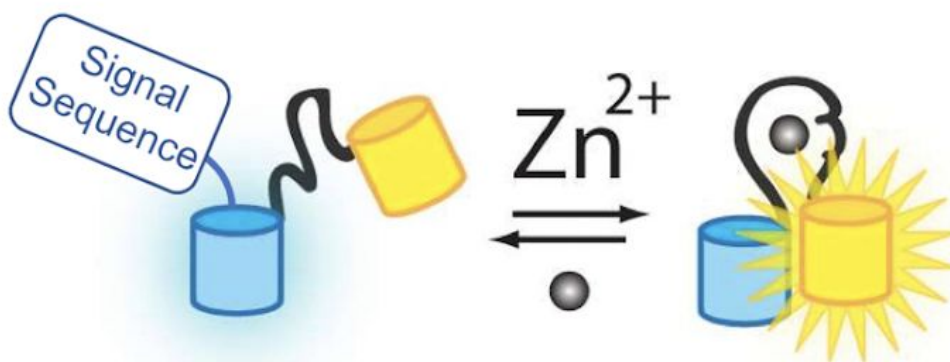

Figure 2: FRET Sensor Zap-CV2 Binding to Labile Zn^{2+} This schematic illustrates the bound and unbound states of the Zap-CV2 sensor. The sensor is comprised of a CFP domain (cyan cylinder) linked to a YFP domain (yellow cylinder) via a Zn^{2+} binding domain (black line). Binding of Zn^{2+} results in a conformational change resulting in a change in fluorescence from CFP to YFP. *Figure provided courtesy of Leah Damon.*

Thesis aims

This study aims to determine how knockdown of MTF-1 alters proliferation, zinc buffering and the tolerance of these cells to zinc deficient conditions. In order to accomplish this, I utilized fluorescence microscopy in order to quantify the amount of labile Zn^{2+} in both MTF-1 knockdown and control mammary epithelial MCF10A cell lines. I then conducted proliferation assays to compare cellular proliferation in both zinc replete and deplete conditions. My hypothesis was that since MTF-1 is known to be a transcription factor for the ZnT1, ZnT2 and metallothionein genes, knockdown of MTF-1 would result in a reduced ability of the cell to create more of these proteins, resulting in an increase in labile cytosolic Zn^{2+}. I further speculate that this would result in decreased cellular proliferation when exposed to high concentrations of Zn^{2+}, as the cell would now essentially be in a diseased state, with unhealthy levels of Zn^{2+}.

However, when the cell is in zinc deficient conditions, I postulate that there would be little to no difference between the knockout cell line versus the control, as the current understanding of MTF-1 reflects that it is primarily implicated in Zn^{2+} export and sequestration - not import. I also replicated the knockdown of the MTF-1 gene with the intention of repeating experiments with the new cell lines in order to ensure that the results of the imaging experiments were iterative.

Materials and Methods

Reagents

Reagent type	Designation	Source or reference
Plasmid	pREV	Palmer lab
Plasmid	psPAX2	Addgene Cat. #: 12260
Plasmid	pMD2.G	Addgene Cat. #: 12259
Cell line (*H. sapiens*)	MCF10A + NES-ZapCV2	Published in previous Palmer lab paper PMID: 27959493
Cell line (*H. sapiens*)	MCF10A + NES-ZapCV2 MTF-1 KD	Created by Dr. Maria Lo from above cell line
Cell line (*H. sapiens*)	HEK 293-T cells	ATCC CRL-3216
Antibody	anti-MTF1 (rabbit)	Novus Biologicals NBP1-86380
Antibody	histone H2B (D2H6) Rabbit	Cell Signaling Technology, mAb #12364
Antibody	goat anti-Rabbit IgG (H+L)	Novus Biotechnology NB7160

Cell Culture

MCF10A cells containing NES-ZapCV2 were grown and maintained in 10 cm dishes with 10mL full growth DMEM/F12 medium (FGM) supplemented with 5% horse serum, 1% Pen/strep antibiotics, 20 ng/mL EGF, 0.5 μg/ml hydrocortisone, 100 ng/ml cholera toxin, and 10 μg/ml insulin and incubated at 37° C and 5% CO_2. When the cells were observed to be covering around 80% of the surface area of the dish (80% confluency), they were passaged.

Passaging entails re-plating a small amount of the current cells in a new dish, giving them more room to grow. During passaging, the media is aspirated off of the dish. The cells are then washed with phosphate buffered saline (PBS) to remove any excess media and dead cells. 5 mL of trypsin-EDTA is added to the dish in order to detach the cells from the bottom of the plate. The plate is incubated at 37° C and 5% CO_2 until the cells are detached (around 15 minutes). The trypsin is then neutralized with 5 mL supplemented FGM and the cells are removed from the plate, and the solution is centrifuged at 1,000 RPM for 5 minutes in order to form a cell pellet. The excess media is aspirated off, and the cells are resuspended in 1 mL

supplemented FGM. 100μL of the resuspension is added to a new 10cm dish containing 10 mL supplemented FGM, and the cells are returned to the incubator to grow.

In order to control the concentration of Zn^{2+} in media for analysis, minimal media (MM) was created. MM contains just enough Zn^{2+} for cellular processes to not be negatively impacted (1.8 μM Zn^{2+}) and contains: 50:50 Ham's F12 phenol red free/FluoroBrite DMEM with 1.5% Chelex 100-treated horse serum, 1% Pen/strep antibiotics, 20 ng/mL EGF, 0.5 μg/ml hydrocortisone, 100 ng/ml cholera toxin, and 10 μg/ml Chelex 100-treated insulin. To create a Zinc-deficient condition (ZD), either 2 or 3 μM of membrane permeable zinc chelator Tris(2-pyridylmethyl)amine (TPA) was added to MM (2 ZD and 3 ZD). To create a Zinc-replete (ZR) condition, 30 μM $ZnCl_2$ was added to MM.

HEK293T cells for lentiviral transduction were grown and maintained in 10 cm dishes with 10 mL HEK media (created with 450 mL DMEM, 50 mL FBS & 5 mL Pen-Strep). When the cells were observed to be 80% confluent, they were passaged as stated above, but the cell detachment period is much shorter (~5 minutes).

Live cell imaging

MCF10A cells were transferred into MM in order to determine the labile concentrations of Zn^{2+}. This condition will serve as R_{rest}. To obtain a minimum value for the sensor (R_{min}) as well as a maximum value (R_{max}), imaging media were made as detailed below the day of each imaging experiment. These media were used for in situ calibrations to determine the concentration of Zn^{2+} in cells.

Imaging Media	Reagents
R_{min} (2X)	MM + 50 μL 100 μM TPA[1]
R_{max} (2X, 10 mL)	MM + 100 μL A2 buffer + 100 μL B2 buffer + 30 μL pyrithione + 2 mL 0.1% saponin
A2	Buffer solution containing 2 mM Zn^{2+}, 4 mM Sr^{2+}, 2 mM EGTA[2]
B2	Buffer solution containing 4 mM Sr^{2+}, 2 mM EGTA

Table 1: Creation of live cell imaging media The reagents used to observe minimal (R_{min}) and maximal (R_{max}) sensor capabilities. These components were added to MM the day of each imaging experiment. Each of these media were 2X concentrations as they were added to 1 mL of MM already present in the sample. [1]Tris(2-pyridylmethyl)amine, membrane permeable chelator [2]Ethylene glycol-bis(β-aminoethyl ether)-N,N,N′,N′-tetraacetic acid, chelator.

Live cell imaging was conducted on a Nikon Ti-E inverted microscope equipped with an environmental chamber (Okolab Cage Incubator) to maintain the microscope environment at 37°C, 0% CO_2, and 90% humidity. Images were collected via Nikon Elements software. ROI (regions of interest) were randomly selected in the cytosol of cells so that there were approximately 8-10 ROI for each dish imaged. An additional ROI was placed where there were no cells in order to conduct background subtraction for more accurate calculations. The following fluorescence channels were collected: CFP(excitation)-YFP FRET(emission) (200ms

exposure), YFP(excitation, emission) (200ms exposure), and CFP (excitation, emission) (200ms exposure). Calibration of the sensor was conducted by imaging the cells in MM every 30s for approximately 5 minutes. The imaging was paused, and 1 mL (50%) of media was removed. 2X R_{min} solution was then added to create the Zinc-deficient condition (final concentration 50 μM TPA). The R_{min} condition was imaged every 30s for approximately 5 minutes. The imaging was paused again, and all media on cells was removed, followed by 3 washes of MM in order to remove as much TPA as possible. 1 mL MM and 1 mL R_{max} were added to the cells, and then imaging was resumed taking an image every 10 seconds for approximately 2 minutes, before excessive cell death occurred. Each imaging experiment was replicated at least in triplicate for both knockdown and scrambled control cell lines. A sample trace of this process is provided in **Figure 3**.
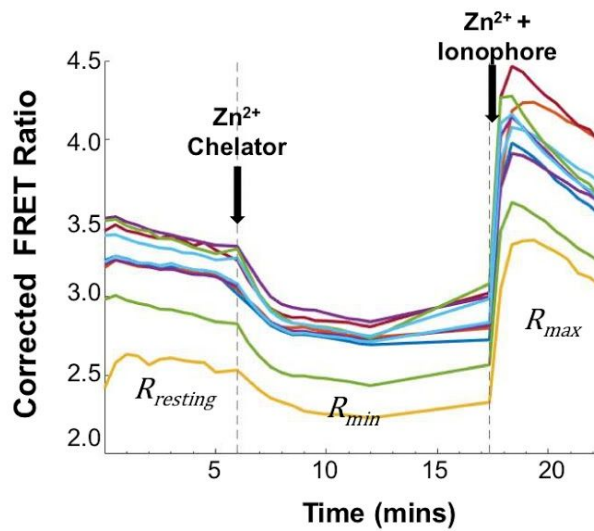

Figure 3: In situ calibration of Zn²⁺ sensor An example of traces obtained from live cell imaging of MCF10A cells. Each trace represents a ROI in a different cell. The FRET ratio is defined as the background corrected FRET signal divided by the background corrected CFP signal. An initial background is taken to represent the resting FRET levels ($R_{Resting}$), then upon addition of chelator TPA the FRET ratio drops, representing the minimum value the sensor can achieve (R_{Min}). Subsequently Zn²⁺ is added back into solution causing the FRET ratio to increase well above the baseline amount, resulting in the maximum value the sensor can achieve, or R_{max}. *Image via Maria Lo.*

Live Cell Imaging Calculations

From the raw live cell imaging data, the resting concentration of labile Zn²⁺ for each cell was estimated via the following equation, where each measured value has been background subtracted:

$$[Zn^{2+}] = K_D \left(\frac{R_{resting} - R_{min}}{R_{max} - R_{resting}}\right)^{1/n}$$

The dissociation constant (KD) of the sensor as well as the Hill coefficient (n) for this sensor are known to be 5.3 ± 1.1 nM and 0.29 ± 0.02, respectively (Sanford 2019). $R_{Resting}$ refers to the average FRET ratio at the beginning of the imaging cycle when the cells are in MM. Here the FRET ratio is defined as the background corrected fluorescence intensity in a ROI in the CFP-YFP FRET channel divided by the background corrected fluorescence intensity in the same ROI in the CFP channel. R_{Min} refers to the average FRET ratio in the middle of the imaging cycle, after chelation of Zn^{2+} by TPA. R_{max} refers to the average FRET ratio at the end of the imaging cycle, after addition of saturating amounts of Zn^{2+} along with pyrithione. This equation provides the concentration for just one cell, the concentrations for MTF1 knockdown and scrambled control cell lines were calculated via averaging the values for each of the cells.

Viral Transduction with shRNA to Knockdown MTF1

HEK293T cells were split from a fully confluent dish into 2 new dishes so that 1/10 of the cells were present in each of the new dishes, and incubated at 37° C. The next day, the lentiviral constructs and packaging plasmids were transfected. The lentiviral construct used was pRev. TransIT-LT1 and OptiMEM were warmed in 37° C hot water bath. TransIT was then vortexed, and 36 μL were diluted into 550 μL OptiMEM. The pRev was then combined with packaging plasmids as seen below in 20 μL OptiMEM, with one mixture containing knockdown (KD) shRNA and the other containing a scrambled control (Scr) shRNA:

Construct	Added	Components
pRev	1.73μg	Viral reverse transcriptase
Ps PAX2	4.5μg	Backbone plasmid (gag and pol genes)
Pm D2.G	0.5μg	VSV-G insert (envelope protein)
MTF-1 shRNA	5mg	Plasmid containing shRNA targeted to MTF-1 gene Target sequence: CCAACTCTGTCCTAACTAATA
Scr shRNA	5mg	Plasmid containing non-specific scrambled shRNA Target sequence: n/a

Table 2: Viral Transduction Constructs This table presents each construct used to conduct viral transduction as well as the quantity of the construct added and its components.

Each mixture was added to half of the diluted TransIT and gently vortexed, then incubated for 20 minutes at room temperature. These mixtures were added to the two plates of HEK cells and the cells were incubated at 37° C.

After about 24 hours, the HEK cells' media was changed, and the HEK cells were split so that they would be around 50% confluent the next day and incubated at 37° C. The following day, successful transfection was verified via mCherry fluorescence (a marker within the plasmid), and the viral supernatants were harvested from the HEK cells. This was done by filtering the supernatants through a 0.45 μm syringe PES (polyethersulfone) filter. The normal growth media was removed from two batches of MCF10A cells and replaced with 6 mL fresh media. 3 mL of each viral media was then added to its respective plate of MCF10A cells. Hexadimethrine bromide (polybrene) was added at 9 μg/mL final concentration to the MCF10A cells. The cells were then incubated at 37° C for 48 h. The cells were observed to have been transfected via fluorescence, so the virus-containing cells were selected by the addition of puromycin. The surviving cells were the new MCF10A MTF-1-KD and Scr cell lines (KD and Scr). The new cell lines were verified both phenotypically (via proliferation in different zinc conditions) and with protein expression (via western blot).

Western Blot

MTF-1 expression of the two new cell lines was evaluated via western blotting. Protein from both Scr and KD cells were isolated via RIPA lysis buffer. In order to quantify isolated protein concentration, a BCA (Bicinchoninic Acid) assay was performed. This assay is conducted via adding small amounts of protein and comparing the color change/absorption of varying known protein concentrations. This plate was read with a plate reader and the approximate concentrations of each cell line's isolated proteins were determined.

5x SDS (sodium dodecyl sulfate) loading dye was added to the isolated protein samples, and the protein was denatured via incubation at 95° C for 5 minutes before loading into a 4-20% gradient SDS polyacrylamide gel. 30 μg of isolated protein from each cell line was loaded, and the reaction was run at 120 V for about 1 hour. The protein from the gel was then transferred to a PVDF (polyvinylidene difluoride) membrane. The membrane was cut in half so that the bottom half of the gel containing H2B (histone 2 B) protein was isolated from the top half of the gel containing the larger MTF-1 protein. Both membranes were treated with blotting buffer containing 5% milk in TBS (tris-buffered saline) solution on a rotating incubator at room temperature.

Antibody	Type	Dilution
anti-MTF1 (rabbit)	Primary	1:1000
histone H2B (D2H6) Rabbit	Primary	1:5000
goat anti-Rabbit IgG (H+L)	Secondary	1:10000

Table 3: Western Blot Antibodies This table contains each of the antibodies used for the Western blot, as well as the type of antibody and its dilution.

After 2 hours, the blotting buffer was aspirated off, and the two halves of the membrane were placed in different boxes. Primary antibody anti-MTF1 was added to the MTF-1 membrane, and primary antibody anti-H2B was added to the H2B membrane. These were placed on a rotating incubator and left overnight at 4° C. Following this, the antibodies were

removed from the membranes, and each membrane was subjected to three 10 minute TBST (TBS buffer with 0.1% Tween-20) washes at room temperature. These washes were also conducted on the rotating incubator, and prior TBST washes were removed before adding new TBST. Secondary antibody goat-anti-rabbit was then added to each membrane. These were incubated at room temperature on a rotating incubator for 1 hour. The antibodies were washed away, and the membranes were again subjected to three 10 minute washes as described before. The membranes were then dried, and a 1:1 ratio of luminol enhancer and a stable peroxide solution was applied in order to visualize the presence of bound antibodies. The membrane was exposed to the solution for 5 minutes. Imaging was conducted on a Quantis-2000 gel box.

Proliferation Assay

Scr and KD cells were split as described above in cell culture, however 10 μL each of resuspended cells were removed, combined in a 1:1 ratio with Trypan Blue dye, and counted via Countess cell counter machine. This allowed for calculation to ensure that approximately the same number of cells were plated for each condition. 125,000 cells per well in a 6 well plate were used. For this experiment, KD and Scr cells were exposed to MM, 3μM TPA (3 ZD), 2 μM TPA (2 ZD), and ZR media in triplicate and incubated at 37° C for 48 hours. Each sample was then trypsinized to remove them from the bottom of the plate, and a 1:1 ratio of media was added to neutralize the trypsin. Remaining media on the plate was kept in order to ensure the dead cell count was accurate. The combination of dead and live cells were centrifuged at 1,000 RPM for 5 minutes in order to form a cell pellet. Excess media was aspirated off and cells were resuspended in 1 mL of FGM. 10 μL from each sample was taken and combined with Trypan Blue dye and live/dead cell counts were measured via Countess cell counter machine.

Results and Analysis

Higher Concentration of Cytosolic Zn^{2+} found in Knockdown Cells

In order to determine the effect of MTF-1 knockdown on labile Zn^{2+} concentration, fluorescence microscopy was conducted. The concentration of labile Zn^{2+} was calculated based on the FRET ratio of bound sensor to unbound sensor in resting, chelated Zn^{2+}, and 30 μM Zn^{2+} conditions. The concentration of labile Zn^{2+} was calculated via utilizing the sensor's maximum and minimum fluorescence values, as well as dissociation constant (Kd) and Hill coefficient (n) as detailed in materials and methods. Based on these calculations, the MTF-1 knockdown cells had a significantly higher concentration of labile Zn^{2+}. For the scrambled cell line the average Zn^{2+} concentration was 37.5 pM ± 7.57, and the average Zn^{2+} concentration for the knockdown cell line was 439 pM ± 77.5 (**Figure 4**). This result makes sense based on what is known about MTF-1, as knockdown of this gene should result in a decrease in labile Zn^{2+} export, resulting in a higher concentration of Zn^{2+} within the cell.

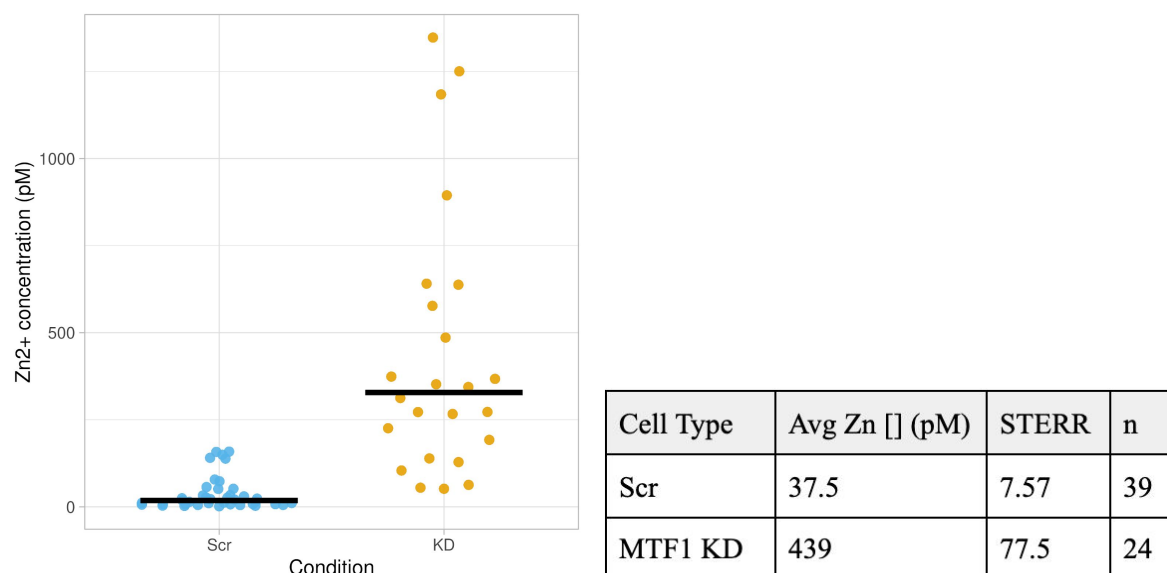| Cell Type	Avg Zn [] (pM)	STERR	n
Scr	37.5	7.57	39
MTF1 KD	439	77.5	24

Figure 4: Calculated Labile Zn Concentrations via Sensor Calibration KD and Scr MCF10A cell lines were imaged, and their background corrected FRET ratios, and then the concentration of labile Zn^{2+} were calculated. This analysis contains data from 3 separate imaging sessions containing a total of 39 scrambled and 24 knockdown cells analyzed. In the dot plot, each blue dot represents the calculated zinc concentration of one Scr cell, while each yellow dot represents the calculated zinc concentration of one KD cell. The average zinc concentration for the scrambled cell line was 37.5 pM ± 7.57, and the average Zn^{2+} concentration for the knockdown cell line was 439 pM ± 77.5. Data analysis via student's two tailed t-Test resulted in $p = 1.3 \times 10^{-8} < 0.05$. *Dot plot generated using PlotsOfData (Postma 2019).*

MTF-1 Knockdown Decreased Proliferation and Increased Cell Death

Once it was established that knockdown of MTF-1 resulted in higher labile Zn^{2+} concentrations, the next question was what effect, if any, does this increase in labile Zn^{2+} have on

the survival of these cells? In order to determine this, a proliferation assay was performed via plating the same initial concentration of cells in resting, chelated Zn^{2+}, and 30 µM Zn^{2+} conditions. These data were visualized in two ways: live cell count to measure proliferation, and percentage of dead cells to measure cell death (**Figure 5**). A one-way ANOVA post hoc T test was performed to identify significant differences in Scr versus KD for each condition. **Figure 5A** shows the live cell count for KD and Scr cells in different media. In both ZD conditions (3 µM and 2 µM), there was a significant decrease in the number of live cells compared to MM. This was expected because the Palmer Lab previously showed that ZD blocks cell proliferation. However, there was no significant difference in the percentage of live cells between KD and Scr cells, indicating that under ZD conditions, the amount of proliferation between the KD and Scr cells was similar. In both MM and ZR media, there was a significant decrease in the extent of proliferation for KD cell lines compared to Scr control, with a more profound difference in the ZR condition.

      Figure 5B presents the results for cell death. The ZD condition with 3 µM TPA led to a significant increase in cell death. All other conditions had significantly lower cell death, with little difference between the Scr and KD cell lines. It appears that the ZR condition resulted in an increase in cell death for MTF1 KD cells. These results fit with the current understanding of MTF-1, as only elevated concentrations of labile cytosolic Zn^{2+} should be binding to MTF-1 enough to expose its NLS sequence and enable translocation and gene activation. Therefore, in conditions with normal or decreased levels of Zn^{2+} the knockdown of MTF-1 should be inconsequential to the survival of the cell.

A

Proliferation Assay Live Count
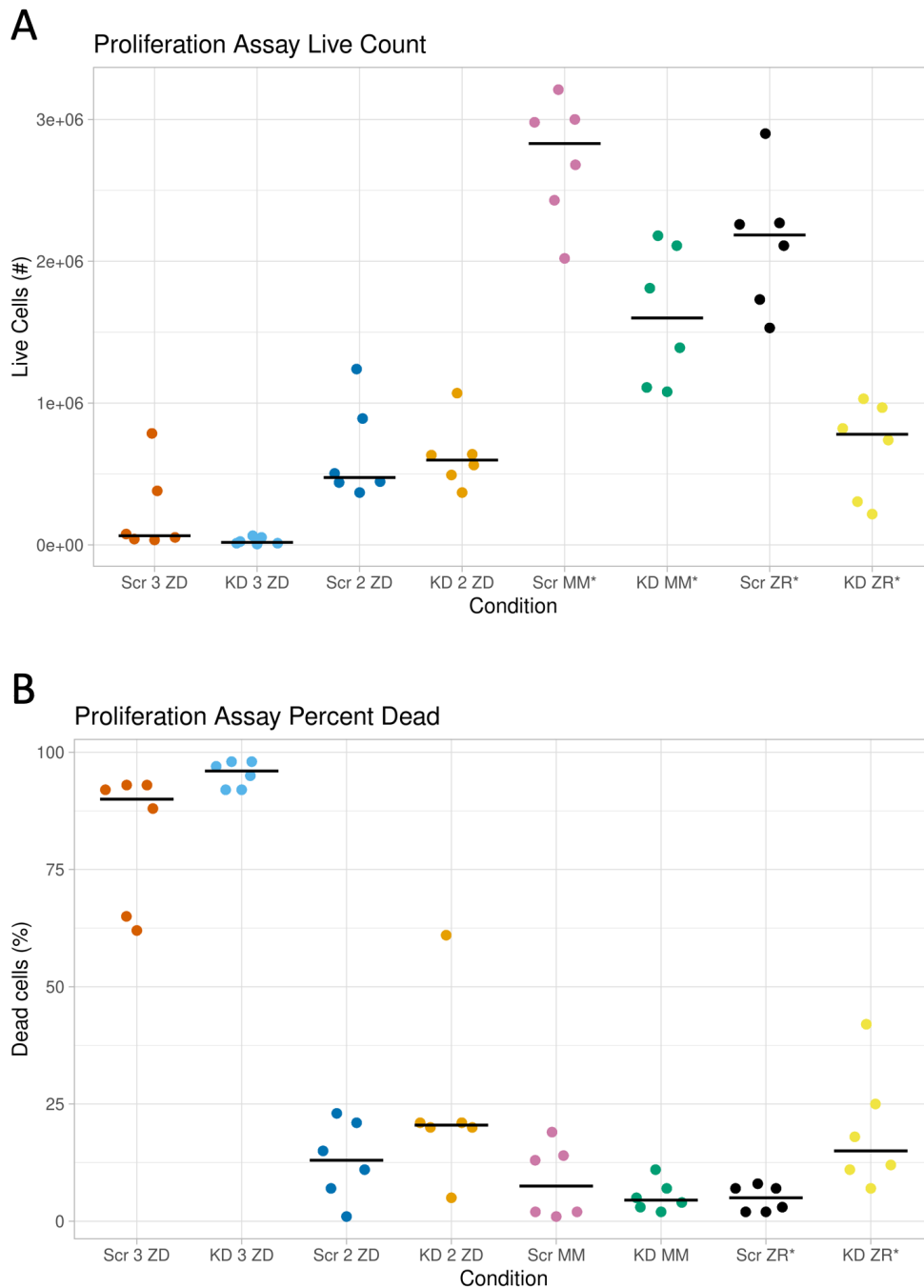
B

Proliferation Assay Percent Dead

Figure 5: Knockdown Cell Line Exhibits Decreased Proliferation and Increased Cell Death
Both KD and Scr cells were plated with same initial concentration, and then were exposed to
3μM TPA (3 ZD), 2 μM TPA (2 ZD), MM or ZR conditions for 48 hours. Live/dead cell counts
were obtained via Countess machine & Trypan Blue dye. In the graphs above, each dot
represents a well of cells counted in its respective condition, and each line represents the median
for each condition. The extent of variance between Scr and KD for each condition was evaluated
via an ANOVA one-way post-hoc t-test. An asterisk (*) designates a significant difference of at

least p < 0.05 between KD and Scr for that condition. (A): The quantity of live cells in each dish across each condition is represented in the graph. There is a significant difference between KD and Scr cell count in both the MM and ZR conditions ($p = 0.0021$ and 0.00012, respectively) (B): The percentage of dead cells compared to live cells in each dish across each condition. Regarding rates of cell death, there is a significant difference between the Scr and KD cells only in the ZR condition ($p = 0.023$). These data are compiled from two independent proliferation assays. *Dot plots generated using PlotsOfData (Postma 2019).*

Successful Knockdown of MTF-1 in MCF10A Cells

   Due to the slightly higher passage number of the original knockdown cell line (~p10-p15) and in an effort to replicate the above results, a new cell line was created via lentiviral transduction. Two different shRNAs (short hairpin RNA) were transduced into NES-ZapCV2 MCF10A cells. One shRNA targeted a region of the MTF-1 gene for knockdown and the other was a non-targeted scrambled shRNA to be used as a negative control. Upon completion of transduction, the decrease in MTF-1 expression was assessed qualitatively by a change in phenotype via fluorescence imaging (**Figure 6**). As shown in Figure 5B, KD of MTF1 led to a significant decrease in cell proliferation in ZR but not MM media so the number cells was evaluated 48 hrs after plating in different growth media. The MTF-1 knockdown cell line proliferated significantly less than the Scr cell line did in 30 μM Zn^{2+} conditions. This suggests that MTF-1 was indeed successfully knocked down, as exposure to increased Zn^{2+} is toxic to the cell when not properly exported. Additionally, the control containing minimal media instead of high concentrations of Zn^{2+} demonstrated significantly more proliferation, on a comparable level to the scrambled condition.
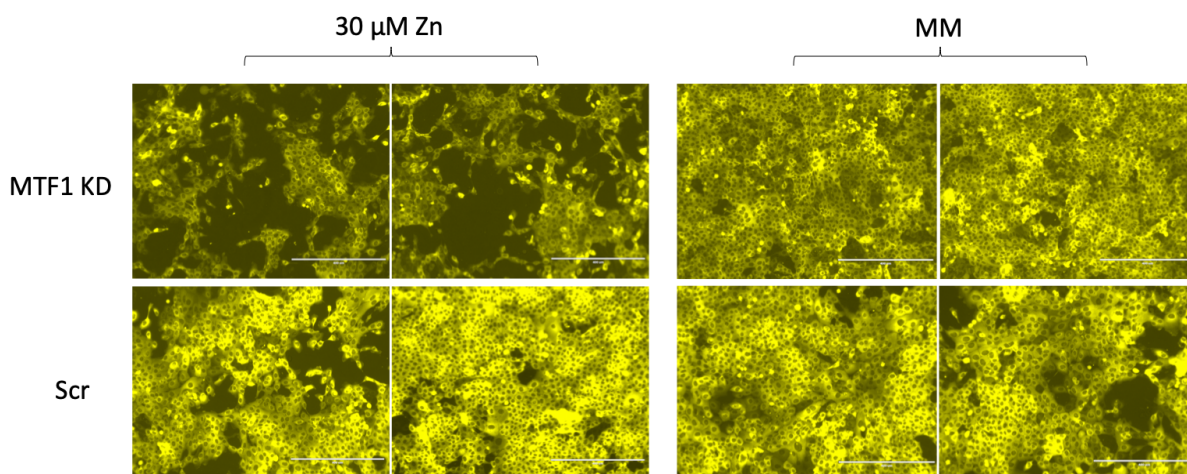

Figure 6: Qualitative Phenotypic MTF-1 Knockdown Confirmation Transfected MCF10A cells (both scrambled and knockdown conditions) were exposed to either minimal media (MM) or 30 μM Zn^{2+} and imaged 48 hours after exposure. Representative fluorescence images are shown in duplicate for each condition. The MTF-1 knockdown cells exhibited significantly less proliferation than the scrambled cell line in 30 μM Zn^{2+} condition, while comparing the two in

minimal media conditions resulted in similar proliferation results. The fluorescent reporter for these images is YFP portion of the Zap-CV2 sensor, and the scale bar is 400 μm.

MTF-1 knockdown was also verified via Western blot analysis (**Figure 7**). Protein was extracted from each cell line, quantified as described in Methods, and an antibody against MTF1 was used to detect the amount of MTF1 protein. H2B was used as a protein control. The KD cell line contained significantly less protein, however it did have noticeably less H2B expressed as well, probably because less protein was loaded in that lane. To control for this, using ImageJ's integral density function, the relative 'darkness' of each of the bands were quantified and background subtracted. The integral densities of each condition were then expressed as a proportion of the H2B control, resulting in the relative expression of each protein. This analysis yielded 41% relative expression in the KD cell line, demonstrating successful knockdown of the MTF-1 gene.
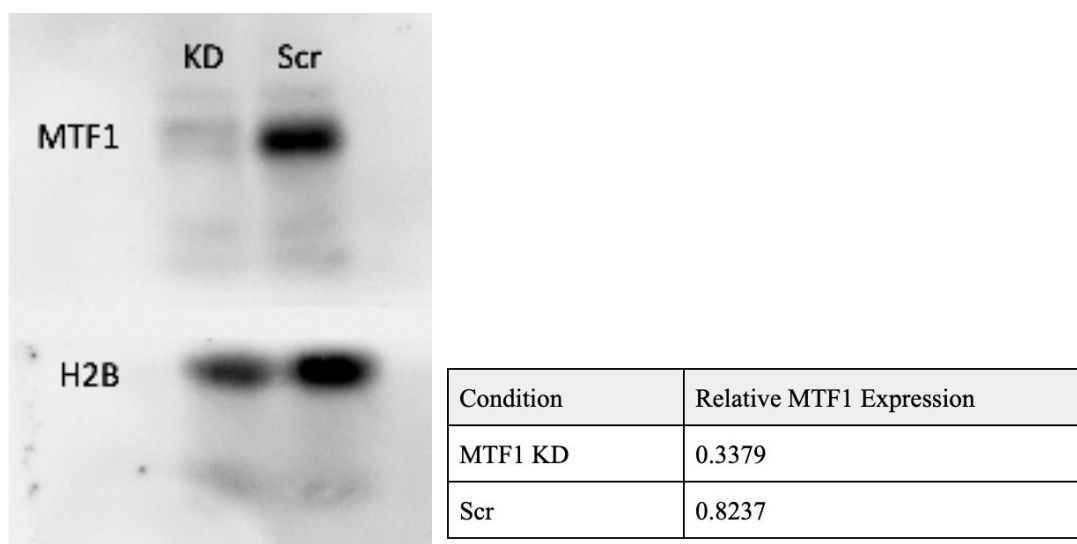

Condition	Relative MTF1 Expression
MTF1 KD	0.3379
Scr	0.8237

Figure 7: Western blot to confirm knock down of MTF1 A Western blot was used to evaluate relative expression of MTF1 in KD and Scr cell lines using antibodies for MTF-1 as well as an H2B control. While the knockdown cell line does contain slightly less H2B, it still demonstrates a significantly decreased expression of the MTF-1 gene when controlled for H2B expression (table).

Discussion

Zinc is the second most abundant transition metal in humans, and it has been proven to be vital for a large number of important cellular processes (Quin 2011, Roohani 2013). Additionally, zinc has been proven to be required for regulation of the cell cycle, and a lack of zinc can induce quiescence (Lo 2020). There are disease states associated with both a lack of zinc ion (Zn^{2+}), such as Parkinson's disease and cancer, and an excess of Zn^{2+}, such as Alzheimer's and chronic kidney disease (Rosa 2019, Zowczak 2001, James 2017, Pelletier 2014). It is clear that it is important to identify what cellular mechanisms exist to regulate zinc, and how deficiencies in these functions could contribute to negative health outcomes. MTF-1 is known to activate when the cell experiences an influx of Zn^{2+} (Gunther 2012). Zn^{2+} binds to MTF-1 allowing it to act as a transcription factor and therefore upregulate the expression of metallothionein, ZnT1, and ZnT2 to sequester and export Zn^{2+} from the cell (Jackson 2020). This thesis aimed to determine how, and to what extent the knockdown of MTF-1 alters cellular proliferation, and zinc buffering.

In order to determine the role of MTF-1 in modulation of Zn^{2+}, this gene was knocked down. With the use of fluorescence microscopy and the NES-ZapCV2 sensor, the MTF-1 knockdown cells had substantially higher (~10x more) cytosolic Zn^{2+} concentrations than the control cells. This is likely due to the fact that MTF-1 activates expression of Zn^{2+} buffering metallothionein as well as of Zn^{2+} exporters ZnT1 and ZnT2. Therefore, knockdown of MTF-1 results in a reduced ability to buffer and export Zn^{2+}, resulting in an overall increase in labile cytosolic Zn^{2+}. Because the process of homeostasis strives to maintain Zn^{2+} concentrations within an optimal range, it seemed plausible that the increased Zn^{2+} might compromise the health of the cell. The rate of proliferation and death upon MTF1 KD were then assessed via incubation for 48h in ZD, MM or ZR media. A significant decrease from Scr to KD was identified in both MM and ZR conditions when looking at cellular proliferation. A significant decrease from Scr to KD was also identified in the ZR condition when looking at the percentage of dead cells. This demonstrates that knockdown of MTF-1 results in decreased cellular proliferation and increased rates of cell death when exposed to higher concentrations of Zn^{2+}. When MTF-1 knockdown was repeated and assessed via Western blot, the KD had a MTF-1 relative expression of 41%, indicating that the KD was successful.

Overall, MTF-1 knockdown in MCF10A cells results in an increase in labile cytosolic Zn^{2+}. Additionally, reduction of the MTF-1 gene results in decreased cellular proliferation in addition to increased rates of cell death in ZR conditions, but no significant difference in proliferation or cell death was observed in ZD conditions. Thus, MTF-1 plays an important role in aiding the cell in tolerating an excess of cytosolic Zn^{2+}, but does not appear to have a role in cellular tolerance of cytosolic Zn^{2+} deficiency. This reinforces what is currently known about MTF-1. MTF-1 activation in excess labile Zn^{2+} conditions results in increased expression in metallothioneins, ZnT1, and ZnT2 in order to better sequester and export Zn^{2+} from the cell.

Future Directions

This thesis set out to demonstrate the effects of MTF-1 knockdown on zinc buffering, cellular proliferation and the tolerance of these cells to zinc deficient and zinc overload conditions. Expanded experimentation using both zinc sensor calibration and proliferation assays would provide a clearer picture of the role of MTF-1. Additionally, zinc sensor calibrations with cells exposed to both ZD and ZR growth media prior to imaging could provide resting zinc concentrations for these conditions, which may further aid the characterization of MTF-1's role in zinc buffering.

Now that this MTF-1 knockdown has been characterized, the role it plays in cell cycle regulation could be further explored. The Palmer lab has found that Zn^{2+} is necessary for both cell cycle regulation as well as induction of quiescence upon Zn^{2+} removal (Lo 2020). Furthermore, fluorescence imaging with the CDK2 reporter could be used to indicate individual cell positions in the cell cycle in MTF-1 knockout cell lines.

Since decreased expression of MTF-1 affects cellular capabilities of buffering and exporting zinc, other avenues can be explored. Increased expression of MTF-1 could aid our understanding of this gene. Hypothetically, overexpression of this gene could result in a decreased cellular sensitivity to excess Zn^{2+}. This could expand the current model of MTF-1's role in cellular processes. While complete knockout of MTF-1 has been conducted in other cells, a full knockout in MCF10A cells specifically could lend a more direct comparison of labile zinc concentrations to knockdown and upregulated conditions (Ji 2018, He 2011). Additionally, the utilization of Zap-CV2 sensor in a knockout MTF-1 cell line in order to determine cytosolic zinc concentrations could provide new insights into MTF-1's regulation capabilities of Zn^{2+}.

The creation of a new MTF-1 knock down cell line provides an opportunity to determine if the results seen with the higher passage knockdown and scrambled cells are reproducible. Specifically, in this newly generated cell line, are Zn^{2+} levels in the cytosol still higher? It would also be beneficial to confirm quantitatively the decrease in MTF-1 knockdown shRNA cell line versus the scrambled shRNA cell line in both the prior and newly generated cell lines. This could be accomplished via replication of the Western blot with a H2B control.

Additionally, in order to further reveal the mechanism by which MTF-1 aids the cell in zinc buffering and export, it would be interesting to knock down some downstream targets of MTF-1. For example, studying MCF10A's response to knock-down of ZnT1, ZnT2, or metallothionein would reveal which of these factors has the greatest contribution to cellular tolerance of increased zinc concentration.

Lastly, the Zap-CV2 sensor itself could be used in other ways. For example the sensor could be targeted to specific organelles, allowing the measurement of the zinc concentration in regions other than the cytosol and could provide more information regarding zinc level changes in disease states.

Commonly Used Acronyms

Acronym:	Definition:
MCF10A	Non-transformed human mammary epithelial cell line - this is the parent cell line for Scr and KD cells
Zap-CV2	Fluorescent sensor - consists of CFP (Cyan fluorescent protein) linked to YFP (Yellow fluorescent protein) with Zn2+ binding domain in the middle. When Zn2+ binds, sensor fluorescence will shift from CFP to YFP
MTF-1	Metal regulatory transcription factor 1 is a transcription factor activated by binding of labile Zn^{2+}
ZnT	Zinc transporter - responsible for zinc transport across membranes - ZnT1 - transports Zn^{2+} out of the cell directly by forming a channel - ZnT2 - transports Zn^{2+} out of the cytosol by importing excess Zn^{2+} into vesicles
KD	MCF10A cell line created with shRNA (short hairpin RNA) targeted to the MTF-1 gene, resulting in MTF-1 knockdown (KD)
Scr	MCF10A cell line created with nonspecific or 'scrambled' shRNA (short hairpin RNA) as a control for the MTF-1 KD
MM	Minimal media - media used for proliferation assay that has been chelexed to contain the lowest concentration of Zn^{2+} that doesn't interfere with cellular proliferation - 1.5 μM (Lo 2020)
ZD	Zinc Deficient - media/condition in which TPA is utilized in order to chelate any Zn^{2+} present in solution, placing stress on the cell via nutritional deficit
ZR	Zinc Replete - media/condition containing minimal media plus 30 μM Zn^{2+}, placing stress on the cell via excess of metal ion
FRET	Fluorescence resonance energy transfer - a process by which energy is transferred from one fluorophore to another via dipole-dipole interactions, measured via emission

Acknowledgments

I would like to first and foremost thank Dr. Amy Palmer, Dr. Maria Lo, and Leah Damon who served as my mentors throughout the course of this project and provided me with all of the support and guidance necessary for successful completion of this work. I would also like to thank the Palmer Lab, who have helped me grow and develop as a scientist throughout the years.

Additionally, I would like to thank the Undergraduate Research Opportunities Program for providing funding for a portion of this thesis. I would also like to give a special mention to Kelsie Anson for her insights into quantification of western blots.

References

Andreini, Claudia, Banci, Lucia, Bertini, Ivano & Rosato, Antonio. (2006). Counting the Zinc-Proteins Encoded in the human Genome. *Journal of Proteome Research*, 2006, 5, 196-201. https://doi.org/10.1021/pr050361j

Augustine, G. J., Fitzpatrick, D., Hall, W. C., LaMantia, A., Mooney, R. D., Platt, M. L., & White, L. E. (2018). Chapter 4: Ion Channels and Transporters. D. Purves (Author), Neuroscience (6th ed., pp. 65-84). New York, NY: Oxford University Press.

Carpenter, M. C., Lo, M. N., & Palmer, A. E. (2016). Techniques for measuring cellular zinc. *Archives of Biochemistry and Biophysics*, *611*, 20–29. https://doi.org/10.1016/j.abb.2016.08.018

Dean, K. M., Qin, Y., & Palmer, A. E. (2012). Visualizing metal ions in cells: an overview of analytical techniques, approaches, and probes. *Biochimica et biophysica acta*, *1823*(9), 1406–1415. https://doi.org/10.1016/j.bbamcr.2012.04.001

Dong, G., Chen, H., Qi, M., Dou, Y., & Wang, Q. (2015). Balance between metallothionein and metal response element binding transcription factor 1 is mediated by zinc ions (Review). *Molecular Medicine Reports*, 11, 1582-1586. https://doi.org/10.3892/mmr.2014.2969

Fiedler BL, Van Buskirk S, Carter KP, Qin Y, Carpenter MC, Palmer AE, Jimenez R. (2017 Jan 3). Droplet Microfluidic Flow Cytometer For Sorting On Transient Cellular Responses Of Genetically-Encoded Sensors. *Anal Chem. 89(1):711-719. doi: 10.1021/acs.analchem.6b03235. Epub 2016 Dec 13.* 10.1021/acs.analchem.6b03235 PubMed 27959493

Gunther, Viola, Lindert, Uschi, & Schaffner, Walter. (2012 September). The taste of heavy metals: Gene regulation by MTF-1. *BBA- Molecular Cell Research* 1823(9); 1416-1425. https://doi.org/10.1016/j.bbamcr.2012.01.005

He, Ziaoqing, & Ma, Qiang. (2011, April 1). Metal sensing by MTF-1 through its carboxyl-terminal cysteine residues. *Federation of American Societies for Experimental Biology* 25(1). https://doi.org/10.1096/fasebj.25.1_supplement.1090.15

Huang, Liping & Tepaamorndech, Surapun. (2012, April 9). The SLC30 family of zinc transporters - A review of current understanding of their biological and pathophysiological roles. *Molecular Aspects of Medicine* 34(2-3):548-560. https://doi.org/10.1016/j.mam.2012.05.008

Jackson, Abigail C., Liu, Jie, Vallanat, Beena, Jones, Carlton, Nelms, Mark D., Patlewicz, Grace Corton, J. Christopher. (2020 July 6). Identification of novel activators of the metal responsive transcription factor (MTF-1) using a gene expression biomarker in a microarray compendium. *Metallomics* 2020(12);1400-1415. https://doi.org/10.1039/D0MT00071J

James, S. *et. al.* (2017). Iron, Copper, and Zinc Concentration in Aβ Plaques in the APP/PS1 Mouse Model of Alzheimer's Disease Correlates with Metal Levels in the Surrounding Neuropil. *ACS Chemical Neuroscience 8* (3), 629-637. DOI: 10.1021/acschemneuro.6b00362

Jeong, J., & Eide, D. J. (2013). The SLC39 family of zinc transporters. *Molecular aspects of medicine*, *34*(2-3), 612–619. https://doi.org/10.1016/j.mam.2012.05.011

Ji, L., Zhao, G., Zhang, P., Huo, W., Dong, P., Watari, H., Jia, L., Pfeffer, L. M., Yue, J., & Zheng, J. (2018). Knockout of MTF-1 Inhibits the Epithelial to Mesenchymal Transition in Ovarian Cancer Cells. *Journal of Cancer*, *9*(24), 4578–4585. https://doi.org/10.7150/jca.28040

Kocaturk, Pelin A., Akbostanci, M. Cenk, Tan, Funda & Guzin Kavas. (2000). Superoxide dismutase activity and zinc and copper concentrations in Parkinson's disease. *Pathophysiology,* 7(1); 63-67. https://doi.org/10.1016/S0928-4680(00)00030-4:

Lee, S., Hennigar, S. R., Alam, S., Nishida, K., & Kelleher, S. L. (2015). Essential Role for Zinc Transporter 2 (ZnT2)-mediated Zinc Transport in Mammary Gland Development and Function during Lactation. *The Journal of biological chemistry*, *290*(21), 13064–13078. https://doi.org/10.1074/jbc.M115.637439

Lo, Maria N, Damon, Leah J, Tay, Jian Wei, Jia, Shang & Palmer, Amy E. (2020, Feb 4). Single cell analysis reveals multiple requirements for zinc in the mammalian cell cycle. *eLife* 2020;9e51107. https://doi.org/10.7554/eLife.51107

Pelletier, C. C., Koppe, L., Alix, P. M., Kalbacher, E., Croze, M. L., Hadj-Aissa, A., . . . Soulage, C. O. (2014). The relationship between renal function and plasma concentration of the cachectic factor zinc-Alpha2-glycoprotein (ZAG) in adult patients with chronic kidney disease. *PLoS One, 9*(7) doi:http://dx.doi.org.colorado.idm.oclc.org/10.1371/journal.pone.0103475

Postma, Marten & Goedhart, Joachim. (2019 March). PlotsOfData-A web app for visualizing data together with their mummaries. *PLoS Biol* 17(3): e3000202. https://doi.org/10.1371/journal.pbio.3000202

Prasad, Ananda S. (2013 March). Discovery of human Zinc Deficiency: Its Impact on human Health and Disease, *Advances in Nutrition*, 4(2); 176–190. https://doi.org/10.3945/an.112.003210

Quin, Yan, Dittmer, Phillip J., Park, Genevieve, Jansen, Katarina B., & Palmer, Amy E. (2011, May 3). Measuring steady-state and dynamic endoplasmic reticulum and Golgi Zn2+ with genetically encoded sensors. *Proceedings of the National Academy of Sciences in the United States of America* 108(18):7351-7356. https://doi.org/10.1073/pnas.1015686108

Roohani, Nazanin, Hurrell, Richard, Kelishadi, Ryoa & Schulin, Rainer. (2013, February). Zinc and its importance for human health: An integrative review. *Journal of Research in Medical Sciences* 18(2):144-157. PMCID: PMC3724376

Rosa, C., Franca, C., Sérgio, L. V., Carvalho, A., Penna, A., Nogueira, C., . . . Ramalho, A. (2019). Reduction of serum concentrations and synergy between retinol, β-carotene, and zinc according to cancer staging and different treatment modalities prior to radiation therapy in women with breast cancer. *Nutrients, 11*(12), 2953. doi:http://dx.doi.org.colorado.idm.oclc.org/10.3390/nu11122953

Sanford, L., Carpenter, M. C., & Palmer, A. E. (2019). Intracellular Zn2+ transients modulate global gene expression in dissociated rat hippocampal neurons. *Scientific reports*, *9*(1), 9411. https://doi.org/10.1038/s41598-019-45844-2

Sekar, R. B., & Periasamy, A. (2003). Fluorescence resonance energy transfer (FRET) microscopy imaging of live cell protein localizations. *The Journal of cell biology*, *160*(5), 629–633. https://doi.org/10.1083/jcb.200210140

Vallee, Bert L. & Falchuk, Kenneth H. (1993). The biochemical basis of zinc physiology. Physiological Reviews 73(1); 79-118. https://doi.org/10.1152/physrev.1993.73.1.79

Wessells, K. Ryan & Brown, Kenneth H. (2012 November). Estimating the Global Prevalence of Zinc Deficiency: Results Based on Zinc Availability in National Food Supplies and the Prevalence of Stunting. *PLoS One* 7(11). https://doi.org/10.1371/journal.pone.0050568

Zhao, J., Wu, Q., Hu, X. *et al.* (2016). Comparative study of serum zinc concentrations in benign and malignant prostate disease: A Systematic Review and Meta-Analysis. *Sci Rep* 6, 25778. https://doi.org/10.1038/srep25778

Zowczak, M., Iskra, M., Torliński, L. *et al.* (2001). Analysis of serum copper and zinc concentrations in cancer patients. *Biol Trace Elem Res* 82, 1. https://doi-org.colorado.idm.oclc.org/10.1385/BTER:82:1-3:001